Original Article	*Curr. Appl. Sci.*, **2026**, *4*(1): 51-65 DOI: 10.22034/cas.2025.233426	Current Applied Sciences

Investigation of the Mutual Interactions of the Sodium Ion and Some 15-Crown-5 Ethers through an Experimentally Based QSPR Model and Quantum Mechanical Features

Mahmood Sanchooli*, Pouya Karimi, Fereshteh Shiri

Department of Chemistry, Faculty of Science, University of Zabol, Zabol, Iran

Corresponding author's e-mail: *sanchooli@uoz.ac.ir*

Article Information

Received: 12 June 2024
Revised: 06 September 2025
Accepted: 07 September 2025
Published online: 02 November 2025

Keywords

15-Crown-5 ether
Stability constant
QSPR
Orbital energies
Electronic descriptors

Abstract

The mutual interactions between the sodium ion (Na^+) and hydrogen, carbon and oxygen atoms of the rings of a number of 15-crown-5 ether (15C5) derivatives were explored. Three different categories of descriptors including dipole moments, orbital energies and atomic charges were obtained from quantum mechanical calculations. A reliable correlation between stability constant (logK) of the 15C5 ethers and the mentioned electronic features was constructed. The model reveals considerable contributions of the C_8 and C_9 atoms in comparison to the other atoms in the rings. Moreover, quantum mechanical calculations confirmed the role of these two carbon atoms on the stability of the structures. Furthermore, a quantitative structure property relationship (QSPR) model was conducted on stability constant values of the mentioned complexes. Furthermore, it is found that a significant electron charge density has condensed between the hydrogen atoms of the rings and sodium ion. Also, ionic character of the interactions between the sodium ion and oxygen atoms of the ring was verified.

1. Introduction

Since the discovery of the crown ethers, they have been subject of a wide variety of research studies [1-8] and received much attention in a few number of works [9-16]. The photo-responsive crown ethers were synthesized to enforce the conformational change of crown ethers for better photo-control of alkali metal cations (Rb^+, Cs^+, K^+, Na^+) during extraction and transportation [9,10]. The conductance property of crown ethers has been previously studied by some authors. They particularly investigated the change in conductance as the crown binds to H^+, Li^+, Na^+, K^+ cations. Thus, the crown ethers act as molecular sensors or molecular switches [11]. It has been found that the cationic binding significantly leads to decrease of conductance due to the quantum mechanical effects.

These macro-cycles are found to be useful in ionic chromatography for determination of the alkali and alkali-earth cations, ammonium, and amines [12]. The fluorescence characters of the mentioned macro-cycles have been investigated via time resolved-emission studies and results showed that the fluorescence gets quenched due to efficient spin-orbit coupling correlations [13]. Moreover, charge transfer in the presence of surfactants, complexation with sodium ions in water-organic solvent mixtures, and effect of benzo substitution on the complexation with $NaClO_4$ have been investigated [14-16].

Crown ethers are capable of reducing the cation/anion interactions through shielding the cations and activating the anions. This property has enhanced the use of crown ethers as a salt solvent in organic solutions and as catalysts in phase-transfer catalysis or enzyme mimics. It can be deduced that the important feature of the crowns is complexation with the cations and in particular with the alkali metal ions. Thus, a broad range of research studies were performed on crown ethers including complexation with the various kinds of cations [17-21]. Different types of interactions influence on the kinetics and thermodynamics of the complex formation in crown ethers in both aqueous and organic solutions [22-29]. Experimental measurement techniques such as potentiometry, conductometry and calorimetry are available to evaluate the stability constants of the complexes of crown ethers with metal ion [30, 31].

Some researchers such as Ghasemi *et al.* developed a QSPR model and determined stability constants for complexes of 15C5 ethers with potassium cation (K^+) at 25 ℃ in methanol solution. They calculated comprehensive descriptors for structural and statistical analysis (CODESSA), including constitutional, geometrical, topological, electronic, thermodynamic and quantum chemical, by applying a semi-empirical quantum computation of Austin Method 1 (AM1) [32]. Shahin Ahmadi et al. investigated stability constants of 65 complexes of 15C5 with sodium ion (Na+) using genetic algorithm based multiple linear regression method [33]. They used dragon software and obtained a collection of classical descriptors to develop a reliable QSPR model. Their QSPR model developed in this study and showed accurate predictions with the leave one out cross-validated variance ($Q^2_{loo} = 0.88$) and the external-validated variance ($Q^2_{ext} = 0.82$). Although in both recent studies that performed on the prediction of stability constants of 15C5 ethers with the potassium and sodium ions the good models were presented, the nature and amount of interactions between cations and crown ether have not clearly been demonstrated. This type of ambiguity, in particular, can be seen in those models which are designed and built using descriptors obtained from dragon software. In order to get a better picture from the 15C5-Na^+ interactions, more relevant quantum mechanical *ab initio* descriptors need to be employed to construct a suitable model.

Since the variation in an activity/property typically will be related to more than one single descriptor, QSAR modeling depends deeply on statistical methods. However, since QSAR modeling may look for unknown relations between several descriptors, traditional statistical approaches such as simple multiple linear regression (MLR) may not be the ideal choice. Thus, development of QSAR models has been often successful in conjunction with a nonlinear regression such as support vector machine (SVM). The SVM introduced by Cortes and Vapnik [34] is a valuable tool for solving pattern recognition and classification problem. The SVM can be employed for regression problems with the introduction of an alternative loss function. The least squares support vector machines (LS-SVM) are an alternate formulation of SVM that was described by Suykens and Vandewalle [35]. The LS-SVM can resolve linear and non-linear multivariate calibration problems in a relatively fast manner. The theory of LS-SVM has also been formerly described [36] and applications of LS-SVM in quantification and classification have been also reported [37, 38].

Herein, we are aiming to explore the effective interactions between the sodium ion and some 15-crown-5 ether derivatives using quantum mechanical calculation based on the experimental results. Indeed, a QSPR model was conducted on stability constant (logK) values of a number of 15C5-Na^+ complexes. A reliable model was constructed using three different categories of descriptors including dipole moments, orbital energies, and atomic charges.

2. Materials and Methods

2.1 *Data set and ligand optimization*

A typical structure of the 15C5 derivatives, shown in the Figure 1, and their corresponding stability constants are taken from the literature [22, 33]. The full structures of the 65 15C5 derivatives that have used in this work are available [33] and for saving space haven't presented. The numerical values of $logK_{exp}$, taken from the literature [33], as well as 24 calculated electronic descriptors for each derivative, are provided in (Supporting Information 1). The molecular structures were built using GaussView 5 and optimized by means of Gaussian 09 at 6-31G(d, p) basis set for all atoms without applying any symmetry constraint.

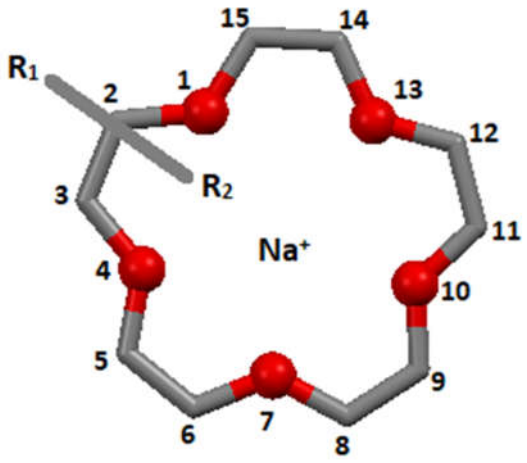

Figure 1. Typical structure of the 15C5 ether-Na^+ complex; only the carbon and oxygen atoms of the ring have numbered

2.2 *Molecular descriptors generation*

A total of 24 molecular descriptors of different types, based on the 3D structure, were calculated to describe the compound structural diversity. Hardness HD, softness SOF, electronegativity EN, and electrophilicity EPH, are the important electronic features used to describe stability, reactivity, chemical potential and other related properties of molecules. Hardness has been used to understand chemical reactivity and stability of molecules [39]. Electronegativity was introduced by Pauling as a power of an atom in a molecule to attract electron toward itself. Softness is a property of a molecule that measures the extent of chemical reactivity. Electrophilicity was proposed by Parr et al. [39] as a measure of energy lowering due to maximal electron flow between donor and acceptor. Taking into account ionization potential $(I) \approx -E_{HOMO}$ and electron affinity $(A) \approx -E_{LUMO}$, the quantum chemical indices of HD, SOF, EN, and EPH can be calculated as HD = $(I-A)/2 = (E_{LUMO}-E_{HOMO})/2$, EN= $(I+A)/2 = -(E_{LUMO}+E_{HOMO})/2$, SOF = 1/HD, and EPH = $(-EN)^2/(2HD)$ [41, 42]. In order to take the contribution of columbic

interactions into account, electrostatic charge values located on i-th either carbon or oxygen atom in the ring of the crown ether (Q_{Ci} or Q_{Oi}), are outlined. Dipole interactions were also characterized using their most relevant total (D_{tot}) and root mean square values (D_{rms}).

The descriptors can be classified into three different electronic categories including dipoles (D_{tot}, D_{rms}), orbital energies (HOMO, LUMO, HD, SOF, EN, EPH) and charges (Q_{Ci}, Q_{Oi}). For each molecule, 24 electronic descriptors were calculated. Therefore, the data matrix contains 65 rows of molecules and 24 columns of electronic descriptors.

2.3 *Variable selection and model building*

The SPSS software, (SPSS Ver. 16, SPSS Inc.), performed MLR analysis and variable selection by using the stepwise method for the variable selection and modeling. This software was applied to the input set of 24 molecular descriptors for each chemical compound and the related response. Then, the best set of molecular descriptors, which are in combination with the most relevant variables in modeling the response of the training set chemicals was extracted using the SPSS software. The selected variables, their numerical value, are provided in Table S2, were used as input for the least square support vector regression ((LS-SVM). Notably, The LS-SVM optimization and model results were obtained using the LS-SVM lab toolbox version 1.5 (MATLAB toolbox for LS-SVM) and other calculations were performed in the MATLAB environment.

2.4 *Least square support vector regression*

The least square support vector regression (LS-SVM) [33] fits a linear relation ($y = wx + b$) between the regression (x) and the dependent variable (y). The best relation is the one that minimizes the cost function (Q) containing a penalized regression (e_i) error term:

$$Q = \frac{1}{2}W^T W + \frac{1}{2}\gamma \sum_{i=1}^{n} e_i^2 \quad (1)$$

Subject to:

$$y_i = W^T \emptyset x_i + b + e_i i = 1, \ldots, n \quad (2)$$

where $\emptyset$ denotes the feature map. The first part of this cost function is a weight decay, which is used to regularize weight sizes and penalize large weights. Due to this regularization, the weights converge to similar value. The large weights deteriorate the generalization ability of the LS-SVM because they can cause excessive variation. The second part of the cost function is the regression error for all training data. The relative weight of this part in comparison to the first part was indicated by the parameter γ, which should be optimized by the user. Similar to other multivariate statistical models, the performance of LSSVMs for quantitative depends on the combination of several parameters. The attainment of the kernel function is cumbersome and it will depend on each case. However, the kernel function more used is the radial basis function (RBF), $\exp\left(-\|x_i - x_j\|^2/2\sigma^2\right)$, a simple Gaussian function, and polynomial functions $(x_i, x_j)^d$, where σ^2 is the width of the Gaussian function and d is the polynomial degree, which should be optimized by the user, to obtain the support vector, for σ of the RBF kernel and d of the polynomial kernel. To achieve a good generalized model, care should be done by user while making a model selection in combination with the regularization constant.

2.5 *Model validation*

Cross-validation as an internal validation method was used to assess the predictive quality of the models. In a standard internal validation method, named LOOCV (leave one out cross-validation), one compound is omitted from the original training set, and a new model is constructed based on the new training set and this model is used to predict the activity of the omitted one. For each model, this process is repeated for whole compounds of the data set, and each compound has been excluded once, then cross-validated q^2 which is considered as a criterion of robustness and predictive ability of the models, was calculated by Eq. (3) [42] as follow:

$$q^2 = 1 - \frac{\sum(y_i - \hat{y})^2}{\sum(y_i - \bar{y})^2} \quad (3)$$

Where $\bar{y}$ presents the average activity value of the entire data set and y_i and $\hat{y}$ are observed and predicted activity values, respectively. A high q^2 value ($q^2 > 0.5$) is used as an evidence of the high predictive ability of the model [43]. Golbarikh and Tropsha reported that the high value of q^2 is essential and important, but not adequate for a predictive model and an external analysis of the test set of molecules should be employed to investigate the prediction of the model.

On the other hand, for the evaluation of the predictive ability of a multivariate calibration model, we generally use the squared correlation coefficient of the experimental vs. predicted activities for test set (R^2_{pred}), root mean square error of prediction set (RMSEP). They are calculated using the following equations.

$$R^2_{pred} = 1 - \frac{\sum_{i=1}^{n}(y_{pred} - y_{exp})}{\sum_{i=1}^{n}(y_{exp} - y_{mean})} \quad (4)$$

$$RMSEP = \sqrt{\frac{\sum_{i=1}^{n}(y_{pred} - y_{exp})}{n}} \quad (5)$$

Golbarikh and Tropsha reported an external analysis of the test set of molecules should be employed to investigate the prediction of the model [44]. They have discussed a QSAR model is predictive if it fulfills the following conditions:

$$q^2 \geq 0.5 \quad (6)$$

$$R^2 \geq 0.6 \quad (7)$$

$$\frac{(R^2 - R_0^2)}{R^2} < 0.1 \ \ or \ \ \frac{(R^2 - R_0^{2'})}{R^2} < 0.1 \quad (8)$$

$$0.85 \leq k \leq 1.15 \quad or \ 0.85 \leq k' \leq 1.15 \quad (9)$$

In addition, Roy [45, 46] stated another validation statistical parameter, named modified R^2 (R_m^2) which assesses the predictive ability of a model and is determined as follows:

$$R_m^2 = R^2(1 - \sqrt{|R^2 - R_0^2|} \quad (10)$$

The R_m^2 value more than 0.5 ($R_m^2 > 0.5$) confirms that the model possesses good external prediction ability.

3. Results and Discussion

The data set of 65 dependent variables of experimental logK values versus 24 calculated descriptors (provided in Supporting Information 2) has been split into 50 and 15 compounds for the training and the test set, respectively, by Kennard and Stone algorithm to maximize the diversity of the test set and examine the predictive accuracy of the model when extrapolating outside the training set [47]. The MLR technique was performed on the compounds of the training set. We applied the stepwise variable selection procedure to select only the best combinations of

those descriptors most relevant to obtain models with the highest predictive power for logK [48]. After regression analysis, a few suitable models were obtained among which the best model was selected and was employed for prediction. On the basis of the highest multiple correlation coefficients (R^2) and simplicity of the model, the best equation is selected. This QSPR model for the logK of the compounds includes six molecular descriptors as presented in the following equation:

$$logK = 8.28 + 11.16\ LUMO - 2.34Q_{O1} + 3.85Q_{C15} - 4.64Q_{C11} + 50.89Q_{C9} + 29.68Q_{C8},\ R^2_{train} = 0.64,\ R^2_{test} = 0.58 \quad (11)$$

The statistical parameters R^2 for the training set and R^2_{pred} for test set is found to be 0.64 and 0.58 by MLR model analysis, respectively. The results are listed in Table 1 and graphically shown in Figure 2.

Table 1. Experimental and predicted logK with residual values for the training and test set compounds by MLR and SVM models

			MLR		SVM	
	Compound	Exp.	Pred.	Res.	Pred.	Res.
Train	1	3.27	3.09	-0.18	3.25	0.02
	2	3.2	3.23	0.03	3.16	0.04
	3	3.1	2.88	-0.22	3.06	0.04
	4	3.03	3.07	0.04	3.05	-0.02
	5	3.12	3.29	0.17	3.15	-0.03
	6	2.95	3.31	0.36	2.99	-0.04
	7	3.3	3.23	-0.07	3.26	0.04
	8	3.25	3.15	-0.1	3.08	0.17
	9	2.89	3.16	0.27	3.09	-0.2
	10	3.04	3.07	0.03	3.06	-0.02
	11	2.83	2.81	-0.02	2.79	0.04
	12	2.72	2.79	0.07	2.78	-0.06
	13	3.07	2.82	-0.25	3.03	0.04
	14	3.04	3.13	0.09	3.08	-0.04
	15	3.03	2.85	-0.18	3.01	0.02
	16	3.02	3.03	0.01	2.98	0.04
	17	3	2.97	-0.03	3.04	-0.04
	18	2.97	3.17	0.2	3.01	-0.04
	19	3.05	3.1	0.05	3.09	-0.04
	20	3.13	3.43	0.3	3.17	-0.04
	21	3.04	3.08	0.04	3.08	-0.04
	22	3.09	3.04	-0.05	3.05	0.04
	23	2.79	3.23	0.44	3.03	-0.24
	24	2.91	3.07	0.16	2.95	-0.04
	25	2.92	3.08	0.16	2.96	-0.04
	26	3.88	3.79	-0.09	3.77	0.11
	27	3.88	3.77	-0.11	3.77	0.11
	28	3.73	3.79	0.06	3.77	-0.04
	29	3.87	3.61	-0.26	3.83	0.04
	30	3.89	3.6	-0.29	3.81	0.08
	31	3.87	3.6	-0.27	3.81	0.06
	32	3.48	3.61	0.13	3.83	-0.35
	33	3.54	3.85	0.31	3.79	-0.25
	34	3.75	3.77	0.02	3.77	-0.02
	35	3.89	3.66	-0.23	3.85	0.04
	36	3.58	3.03	-0.55	3.54	0.04
	37	3.79	3.5	-0.29	3.43	0.36
	38	2.74	3.41	0.67	2.78	-0.04
	39	3.9	3.82	-0.08	3.86	0.04
	40	3.91	3.81	-0.1	3.77	0.14
	41	3.71	3.79	0.08	3.75	-0.04

	42	3.56	3.24	-0.32	3.6	-0.04
	43	3.39	3.68	0.29	3.81	-0.42
	44	3.75	3.59	-0.16	3.79	-0.04
	45	2.79	3.32	0.53	2.83	-0.04
	46	3.82	3.59	-0.23	3.79	0.03
	47	3.86	3.59	-0.27	3.79	0.07
	48	3.75	3.59	-0.16	3.79	-0.04
	49	3.34	3.33	-0.01	3.35	-0.01
Test	1	3.2	3.23	0.03	3.16	0.04
	2	3.18	3.23	0.05	3.16	0.02
	3	3.18	3.03	-0.15	3.05	0.13
	4	2.97	2.86	-0.11	2.8	0.17
	5	3	2.99	-0.01	3.08	-0.08
	6	3.14	3.03	-0.11	3.05	0.09
	7	3.22	3.05	-0.17	3.06	0.16
	8	3.23	3.23	0	2.99	0.24
	9	2.82	3.39	0.57	3.21	-0.39
	10	3.57	3.85	0.28	3.79	-0.22
	11	3.88	3.63	-0.25	3.72	0.16
	12	3.42	3.85	0.43	3.79	-0.37
	13	3.75	3.77	0.02	3.77	-0.02
	14	3.62	3.67	0.05	3.79	-0.17
	15	3.09	2.98	-0.11	3.05	0.04

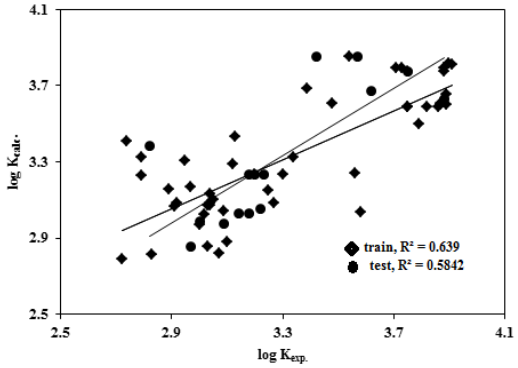

Figure 2. The MLR plot of the calculated versus experimental log K values for training and testing sets of the 65 15C5 derivatives in complexes with Na^+ ion

Due to large residual compound 36 was the outlier and removed from the training set. To improve these statistical parameters, the same set of descriptors was also employed to develop the nonlinear correlation models based on SVM. The experimental versus SVMR-calculated logK values were shown graphically in Figure 3. As Table 2 concerns the relatively high cross-validation q^2(=0.61) value, significantly greater than 0.5, confirms the robustness and predictive ability of the model. For the more verifications on the predictive ability of a multivariate calibration model, the squared correlation coefficient of the experimental vs. predicted properties of the test set (R^2_{pred}=0.70), root means square error of prediction set (RMSEP=0.22) were also presented (see Table 2). In addition to, another validation statistical parameter, named modified R^2 (R^2_m) which assesses the predictive ability of a model, was determined. As shown in Table 2.

$R^2_m = 0.71$, larger than the criteria R_m^2>0.5, confirms that the model possesses good external prediction ability. The other statistical results of SVM model are listed in Table 2. As can be seen from Table 1, the results of the nonlinear model (SVM) are better than those obtained by a linear method (MLR).

Table 2. Statistical parameters of the SVM-based methods

Statistical parameters	
R^2	0.91
q^2	0.61
R^2_{pred}	0.70
RMSEC	0.14
RMSECV	0.27
RMSEP	0.22
$(R^2 - R^2_0)/R^2$	0.001
$(R^2 - R'^2_0)/R^2$	0.00
k	0.992
k'	0.998
R^2_m	0.71

RMSEC: root mean square error of calibration set
RMSECV: root mean square error of cross-validation
RMSEP: root mean square error of prediction set

The equation (11) reveals that the stability constants of the 15C5 series directly depend on lowest unoccupied molecular orbital energies (LUMO) as well as charges located on the C_8.

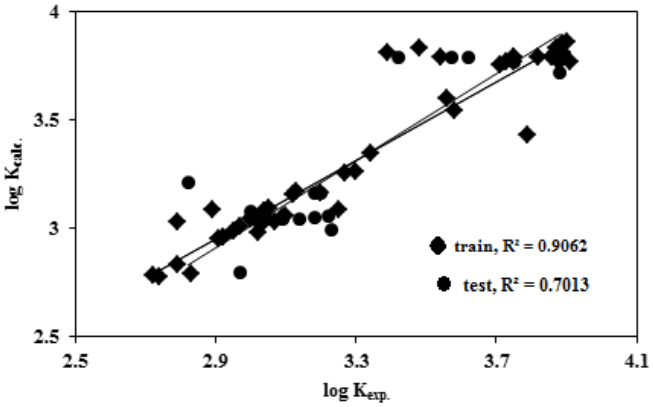

Figure 3. The correlation between calculated and experimental logK values of the 65 15C5 derivatives using Support- vector machine method

C_9, C_{11}, C_{15} and O_1 atoms in the crown ring. It seems that a large LUMO energy value as well as the large positive charge on the C_8, C_9 and C_{15} atoms increases the stability of the complexes.

Similarly, an increase in negative charge on O_1 atom increases the stability of the complexes. However, the concentration of positive charge on C_{11} decreases the stability (see Figure 1). The contribution as well as the relative importance of any involved descriptors to the stability constants, based on the achieved model, was calculated using the following equation and presented in Figure 4.

$$MF_j = \frac{\beta_j \sum_{i=1}^{i=n} d_{ij}}{\sum_j^m \beta_j \sum_i^n d_{ij}} \quad (12)$$

where MF_j represents the mean effect for the under consideration features j, βj is the coefficient of the descriptor j, d_{ij} stands for the value of the target descriptors for each complex and m is the descriptor number in the model. Based on the results shown in Figure 4, the charge located on the C_8 and C_9 considerably affects the stability constants of the complexes. Furthermore, the rest descriptors of LUMO, the charge on O_1 as well as C_{11} and C_{15} slightly contribute to stability constants of the 15C5 complexes with sodium ion. We optimized eleven complexes

of structures **6, 12, 18, 24, 30, 36, 42, 48, 54, 60** and **65** with sodium ion at the HF level of theory using 6-31G(d, p) basis function to provide more verification.

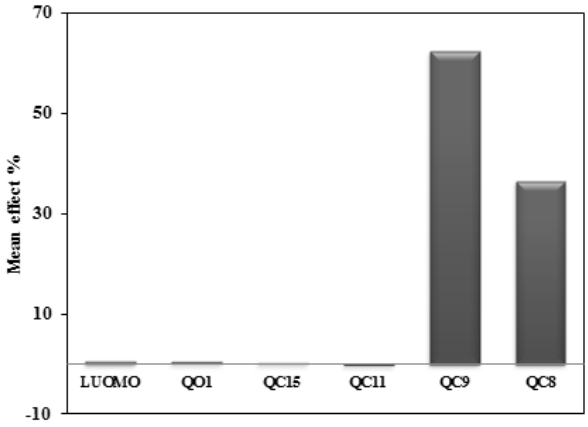

Figure 4. The mean effect percent of any descriptors on calculated log K, based on the model in this work. (Q_{O1}: charge on oxygen 1 in the ring, Q_{C15}: charge on carbon 15, and so forth

The wave functions of the optimized complexes were extracted using Gaussian 09. The atoms in molecules (AIM) method using AIM2000 software was used to analyze and visualize the interaction of the sodium ion with oxygen, carbon and hydrogen atoms in the rings of the 15C5. Molecular graph of compound **6** with sodium ion is presented in Figure 5 as a typical complex. There are concentrated charge densities between sodium ions and the hydrogen atoms of the ring. The AIM results for the ten rest complexes are the same as complex 6. As Figure 5 shows, there exist no critical points between the sodium ion and the oxygen atoms in the ring. Moreover, the charge concentration is rarely found between the cation and the carbon atoms located in the ring. In Table 3, charge densities concentrated between the sodium ion and the hydrogen bearing the carbon atoms in the ring, for all eleven complexes, were listed. Then, efforts were made to construct a correlation between the stability constants logK and the charge densities. As can be seen in Figures 6-8, there are direct correlations between experimental logK values and consecutive carbon atoms.

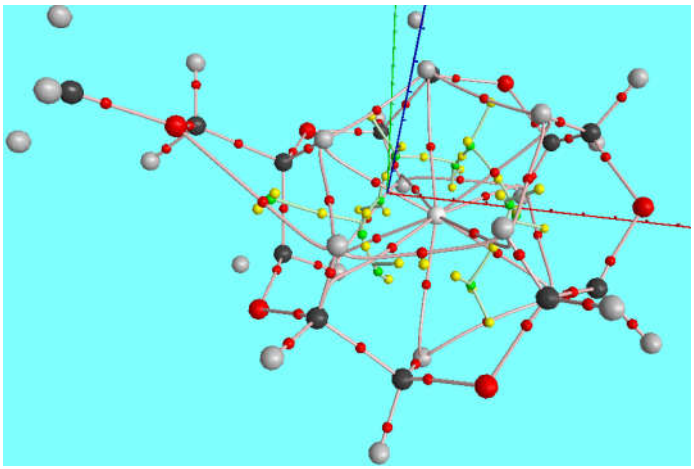

Figure 5. The molecular graph of a usual 15C5 ether-Na^+ complex including bond critical points (red), ring critical points (yellow), and cage critical points (green)

Table 3. Numerical values of charge density of H…Na^+ bond, bearing the carbon atom in the ring of 15C5, for the eleven selected complexes

Entry	ρ (… Na^+)									
	C_2H	C_3H	C_5H	C_6H	C_8H	C_9H	$C_{11}H$	$C_{12}H$	$C_{14}H$	$C_{15}H$
6	0.01265	0.01104	0.00905	0.01108	0.01042	0.01080	0.00937	0.01063	0.00807	0.00970
12	0.01071	0.00955	0.01064	0.01005	0.00981	0.00972	0.00998	0.00948	0.01039	0.01056
18	0.00958	0.01083	0.01052	0.01016	0.00978	0.00962	0.00971	0.00956	0.01043	0.01100
24	0.01244	0.01100	0.01003	0.01105	0.01030[a]	0.01080	0.00964	0.01076	0.00764	0.00907[a]
30	0.00979	0.01052	0.01050	0.01006	0.00988	0.00969	0.01004	0.00953	0.01041[a]	0.01057
36	0.00000[a]	0.01062[a]	0.01159[a]	0.00862[a]	0.01085[a]	0.00833[a]	0.01098[a]	0.00000[a]	0.01151[a]	0.01056[a]
42	0.00000	0.01292	0.01007	0.00817	0.01176	0.00000	0.01119	0.00870	0.01110	0.00901
48	0.00000[a]	0.01191	0.00998	0.00791	0.01076	0.00806	0.01087	0.00795	0.01116	0.01107
54	0.00000	0.01073	0.00945	0.00820	0.01127	0.00927[a]	0.01195	0.00896	0.01144	0.01050
60	0.00000	0.01224	0.01080	0.00000[a]	0.01104	0.00000	0.01108	0.00000[a]	0.01248	0.00974
65	0.00958	0.01066	0.00951	0.01071	0.00962	0.01110	0.00993	0.01113	0.00985	0.01125

[a] Data found as outlaier in the correlation of $\log K_{exp}$ with the charge densities

The aim is to explore the charge density, which more benefits the stability constant. The results are graphically shown in Figure 8. The reasonable correlations were found in the charge density difference between sodium ion and hydrogen bearing two neighboring C_{15}-C_{14}, C_3-C_2 and C_9-C_8 as presented in Figure 8-a, b and c, respectively.

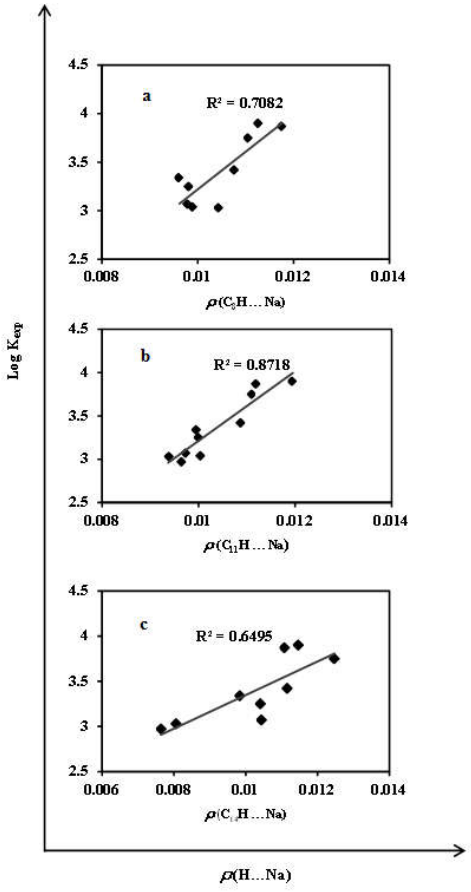

Figure 6. The correlation between log K_{exp} and the charge density of H…Na, bearing C_8 (a) as well as C_{11} (b) and C_{14} (c) atoms in the 15C5 for the 6, 18, 24, 30, 42, 48, 54, 60 and 65 complexes

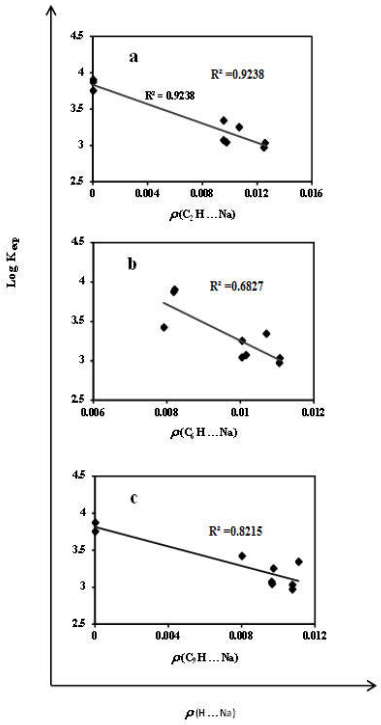

Figure 7. The correlation between log K_{exp} and the charge density of H…Na bond, bearing C_2 (a) as well as C_6 (b) and C_9 (c) atoms in the 15C5 for the 6, 18, 24, 30, 42, 48, 54, 60 and 65 complexes

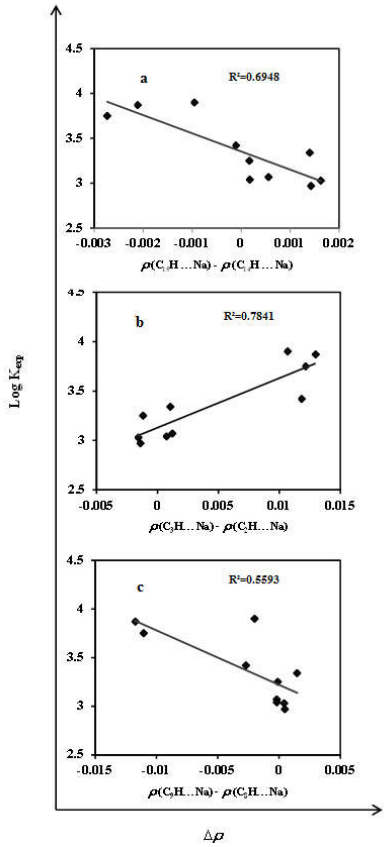

Figure 8. The correlation of log K_{exp} with the charge density difference of H…Na bonds, bearing the two consecutive C_{15}, C_{14} (a) as well as C_3,C_2 (b) and C_9, C_8 (c) atoms in the 15C5 for the 6, 18, 24, 30, 42, 48, 54, 60 and 65 complexes

As can be seen in Figure 8, logK more benefits from the charge density between sodium ion and hydrogen bearing C_{14}, C_3 and C_8, than their neighbor C_{15}, C_2 and C_9, respectively. These might be along with the results proposed by the model indicating that the carbon atoms of C_2, C_{15}, C_8, and C_9 in the ring are involved in the stability constants of the 15C5 series.

4. Conclusion

Three different descriptors explicitly dipole moments, charges, and orbital energies were extracted for any individual 15C5 derivatives. A reliable QSPR model was constructed between stability constants and the electronic classes of descriptors which revealed that the local charge on the carbon atoms, particularly positive charges on the C8 and C9 atoms have prevailing contributions on the stability constants. Furthermore, the model proposes a slight contribution of the LUMO in stability constants. In addition, the further calculations disclosed the presence of the charge densities between hydrogen of the ring and the sodium ion and revealed the lack of chemical bonds between the Na^+ ion and the carbon as well as oxygen atoms of the ring. This may infer the ionic character of interaction between the metal ion and the oxygen as well as carbon atoms of the ring. The fact that the Na^+ ion is fortified at the center of the rings by the hydrogen atoms is also deduced.

Supporting Information Summary

Supplementary data associated with this article (SI1 and SI2) include stability constants of 15-crown-5 ether complexes with sodium cation using *ab initio* calculation in conjunction with a proper QSPR model.

Acknowledgment

We thank the University of Zabol for all supports (Grant number: UOZ-GR-4849).

Conflicts of Interest

The authors declare that there are no conflicts of interest regarding this article.

References

1. Ghildiyal N. Experimental investigations of complexes of some small ring fluorescent benzo oxa-crown ethers with alkali metal ions in solution phase: A review. *J. Mol. Struct.* 2024, 1312, 138603.
2. Ripon RI, Begum ZA, Rahman IMM. Selective separation of radionuclides from aqueous matrices using crown Ether: A review. *Microchem. J.* 2024, 199, 110161.
3. Kim H, Saito N, Kim D. Synthesis of crown-ether-embedded graphene by the solution plasma. *Carbon* 2024, 216, 118578.
4. Ling YH, Yong WW, Bo H, Ling SY, Liang MT, Ran Z. First hyperpolarizabilities of Pt(4-ethynylbenzo-15-crown-5)2(bpy) derivatives with the complexation of mono-cations (Li^+, Na^+, K^+) and di-cations (Mg^{2+}, Ca^{2+}): development of a cation detector. *RSC Adv.* 2017, 7, 41830-41837.
5. Malgorzata J, Longina MK, Michal W, Andrzej J. Effect of temperature and solvent properties on the process of complex formation between crown ether 15C5 and Na^+ in the (propan-1-ol + water) mixture at temperatures from T = 293.15 K to T = 308.15 K. *J. Chem. Thermodyn.* 2017, 113, 321-329.

6. Yoshiya I, Motoki K, Takayuki E. Geometric and Electronic Structures of Dibenzo-15-Crown-5 Complexes with Alkali Metal Ions Studied by UV Photodissociation and UV-UV Hole-Burning Spectroscopy. *J. Phys. Chem. A* 2017, 121, 954-962.
7. Ling YH, Yong WW, Bo H, Ying Z, Ling SY, Qiang HZ. Variational first hyperpolarizabilities of 2,3-naphtho-15-crown-5 ether derivatives with cation-complexing: a potential and selective cation detector. *Phys. Chem. Chem. Phys.* 2016, 18, 26487-26494.
8. Takao M. Maki S, Katsuhiko F. Effects of added salts on adsorbed film and premicelle formation of crown ether surfactants. *Colloids Surf. A* 2015, 482, 447-453.
9. Shinkai S, Nakaji T, Noshihiro Y, Ogawa T, Manabe O. Photoresponsive crown ethers. 1. Cis-Trans Isomerism of Azobenzene as a tool to enforce conformational Changes of crown ethers and Polymers. *J. Am. Chem. Soc.* 1980, 102, 5860-5865.
10. Shinkai S, Nakaji T, Ogawa T, shigematsu K, Manabe O. Photoresponsive crown ethers. 2. Photocontrol of ion extraction and ion transport by bis (crown ether) with a butterfly-like motion. *J. Am. Chem. Soc.* 1981, 103, 111-115.
11. Lui C, Walter D, Neuhauser D. Molecular Recegnition and conductance in crown ethers. *J. Am. Chem. Soc.* 2003, 125, 13936-13937.
12. Izatt RM, Christensen JJ. Synthesis of Macrocycles: The Design of Selective Complexing Agents (Progress in macrocyclic chemistry). New York: John Wiley & Sons Inc. 1987.
13. samanta S, Sardar PS, Pal A, Roy MB. Comparative photophysical behaviour of naphthalene-linked crown ethers and aza crown ethers of varying cavity dimentions. *Chem. Sci. J.* 2007, 119, 175-183.
14. Salman SR, Salem MA, Al-Saadi HA. Molecular complexes of crown ethers. *J. Incl. Phenom. Macrocycl. Chem.* 2002, 42, 289-293.
15. Jóźwiak MŁ. Complex Formation of Crown Ethers with Cations in the Water–Organic Solvent Mixtures. Part VII. Thermodynamic of Interactions of Na^+ Ion with 15-Crown-5 Ether in the Mixture of Water with N,N-Dimethylacetamide at 298.15 K. *J. Incl. Phenom. Macrocycl. Chem.* 2004, 49(3), 303-309.
16. Koylu MZ, Demirel N, Polant FD, Yilmaz A, Hosgoren H, Balci M. The effect of Benzo substitution on complexation of diaza 18-crown-6 ethers derivatives with $NaClO_4$. *J. Incl. Phenom. Macrocycl. Chem.* 2005, 52, 51-54.
17. Tawarah K, Mizyed S. A conductance study of the association of alkali cations with 1,13-dibenzo-24-crown-8 in acetonitrile. *J. Solut. Chem.* 1989, 18, 387-401.
18. Cabbiness DK, Margerum DW. Effect of macrocyclic structures on the rate of formation and dissociation of copper (II) complexes. *J. Am. Chem. Soc.* 1970, 92, 2151-2153.
19. Chen L, Bos M, Grootenhuis P, Christenhusz A, Hoogendam E, Reinhoudt D, Van der Linden W. Stability constants for some divalent metal ion/crown ether complexes in methanol determined by polarography and conductometry. *Anal. Chim. Acta* 1987, 201, 117-125.
20. Mei E, Liu L, Dye JL, Popov AI. Determination of stability constants of cesium [2]-cryptand complexes in nonaqueous solvents by cesium-133 NMR. *J. Solut. Chem.* 1977, 6, 771-778.
21. Mei E, Popov AI, Dye JL. Complexation of the cesium cation by macrocyclic polyethers in various solvents. A cesium-133 nuclear magnetic resonance study of the thermodynamics and kinetics of exchange. *J. Phys. Chem.* 1977, 81, 1677-1681.

22. Izatt RM, Pawlak K, Bradshaw JS, Bruening RL. Thermodynamic and kinetic data for macrocycle interactions with cations and anions. *Chem. Rev.* 1991, 91, 1721-2085.
23. Burger K. Solvation, Ionic and Complex Formation Reactions in Non-Aqueous Solvents-Experimental Methods for their Investigation. Budapest: Akademia Kiado. 1983.
24. Loyola V, Pizer R, Wilkins R. The kinetics of complexing the alkaline-earth ions with several cryptands. *J. Am. Chem. Soc.* 1977, 99, 7185-7188.
25. Monsef Z, Rounaghi G, Sarafraz A. A Polarographic Study of Tl^{+}, Pb^{2+} and Cd^{2+} Complexes with Aza-18-crown-6 and Dibenzopyridino-18-crown-6 in some Binary Mixed Non-aqueous Solvents. *J. Incl. Phenom. Macrocycl. Chem.* 2001, 39, 321-325.
26. Rounaghi G, Yazdi AS, Monsef Z. A Polarographic Study of Tl^{+}, Pb^{2+} and Cd^{2+} Complexes with Dicyclohexano-18-Crown-6 in Some Binary Mixed Solvents. *J. Incl. Phenom. Macrocycl. Chem.* 2002, 43, 231-237.
27. Nezhadali A, Rounaghi G, Chamsaz M. Stoichiometry and stability of complexes formed between 18-crown-6 as well as dibenzo-18-crown-6 ligands and a few metal ions in some non-aqueous binary systems using square wave polarography. *Bull. Korean Chem. Soc.* 2000, 21, 685-689.
28. Ghasemi J, Shamsipur M. A kinetic study of complex formation between calcium ion and cryptand C221 in dimethylsulphoxide solution. *Polyhedron* 1996, 15, 923-927.
29. Alizadeh N, Shamsipur M. Nuclear magnetic resonance study of the ligand interchange of Ba^{2+}-18-crown-6 complex in methanol solution. *J. Solut. Chem.* 1996, 25, 1029-1039.
30. Cox BG, Schneider H. Coordination and transport properties of macrocyclic compounds in solution. Amsterdam: Elsevier Science. 1992.
31. Balzani V, Credi A, Venturi M. Photochemistry and photophysics of coordination compounds: an extended view. *Coord. Chem. Rev.* 1998, 171, 3-16.
32. Ghasemi J, Saaidpour S. QSPR modeling of stability constants of diverse 15-crown-5 ethers complexes using best multiple linear regression. *J. Incl. Phenom. Macrocycl. Chem.* 2008, 60, 339-351.
33. Ahmadi S. Application of GA-MLR method in QSPR modeling of stability constants of diverse 15-crown-5 complexes with sodium cation. *J. Incl. Phenom. Macrocycl. Chem.* 2012, 74, 57-66.
34. Cortes C, Vapnik V. Support-vector networks. *Mach. Learn.* 1995, 20, 273-297.
35. Suykens JA, Vandewalle J. Least squares support vector machine classifiers. *Neural Process. Lett.* 1999, 9, 293-300.
36. Suykens JA, Vandewalle J. Recurrent least squares support vector machines. *IEEE Trans. Circuits Syst. I, Fundam. Theory. Appl.* 2002, 47(7), 1109-1114.
37. Yu K, Cheng Y. Discriminating the genuineness of Chinese medicines using least squares support vector machines. *Chin. J. Anal. Chem.* 2006, 34, 561-564.
38. Khosrokhavar R, Ghasemi JB, Shiri F. 2D quantitative structure-property relationship study of mycotoxins by multiple linear regression and support vector machine. *Int. J. Mol. Sci.* 2010, 11, 3052-3068.
39. Parr RG, Chattaraj PK. Principle of maximum hardness. *J. Am. Chem. Soc.* 1991, 113, 1854-1855.
40. Maksic ZB. Theoretical Models of Chemical Bonding-Part 2-The Concept of the Chemical Bond. Berlin: Springer. 1990.

41. Thanikaivelan P, Subramanian V, Rao JR, Nair BU. Application of quantum chemical descriptor in quantitative structure activity and structure property relationship. *Chem. Phys. Lett.* 2000, 323, 59-70.
42. Wold S. Cross-validatory estimation of the number of components in factor and principal components models. *Technometrics* 1978, 20, 397-405.
43. Hawkins DM, Basak SC, Mills D. Assessing model fit by cross-validation. *J. Chem. Inf. Comput. Sci.* 2003, 43, 579-586.
44. Golbraikh A, Tropsha A. Beware of q 2!. *J. Mol. Graph. Model.* 2002, 20, 269-276.
45. Pratim Roy P, Paul S, Mitra I, Roy K. On two novel parameters for validation of predictive QSAR models. *Molecules* 2009, 14, 1660-1701.
46. Tropsha A, Gramatica P, Gombar VK. The importance of being earnest: validation is the absolute essential for successful application and interpretation of QSPR models. *Mol. Inform.* 2003, 22, 69-77.
47. Kennard RW, Stone LA. Computer aided design of experiments. *Technometrics* 1969, 11, 137-148.
48. Melagraki G, Afantitis A, Sarimveis H, Koutentis PA, Markopoulos J, Igglessi-Markopoulou O. Identification of a series of novel derivatives as potent HCV inhibitors by a ligand-based virtual screening optimized procedure. *Bioorg. Med. Chem.* 2007, 15, 7237-7247.

How to cite this article: Sanchooli M, Karimi P, Shiri F. Investigation of the Mutual Interactions of the Sodium Ion and Some 15-Crown-5 Ethers through an Experimentally Based QSPR Model and Quantum Mechanical Features. *Curr. Appl. Sci.*, 2026, 4(1):51-65. https://doi.org/10.22034/cas.2025.233426